JOURNAL OF GENERAL VIROLOGY

SHORT COMMUNICATION

Ziegler *et al.*, *Journal of General Virology* 2018;99:187–193

DOI 10.1099/jgv.0.001004

MICROBIOLOGY SOCIETY

The use of novel epitope-tagged arenaviruses reveals that Rab5c-positive endosomal membranes are targeted by the LCMV matrix protein

Christopher M. Ziegler,[1,2]† Emily A. Bruce,[1]† Jamie A. Kelly,[1] Benjamin R. King[1,2] and Jason W. Botten[1,3,*]

Abstract

We report the development of recombinant New World (Junín; JUNV) and Old World (lymphocytic choriomeningitis virus; LCMV) mammarenaviruses that encode an HA-tagged matrix protein (Z). These viruses permit the robust affinity purification of Z from infected cells or virions, as well as the detection of Z by immunofluorescent microscopy. Importantly, the HA-tagged viruses grow with wild-type kinetics in a multi-cycle growth assay. Using these viruses, we report a novel description of JUNV Z localization in infected cells, as well as the first description of colocalization between LCMV Z and the GTPase Rab5c. This latter result, when combined with our previous findings that LCMV genome and glycoprotein also colocalize with Rab5c, suggest that LCMV may target Rab5c-positive membranes for preassembly of virus particles prior to budding. The recombinant viruses reported here will provide the field with new tools to better study Z protein functionality and identify key Z protein interactions with host machinery.

Arenaviruses are enveloped, negative-strand RNA viruses that cause severe disease in humans, although their rodent hosts generally remain asymptomatic [1-4]. The arenavirus proteins are highly multifunctional, as every step in the viral life cycle must be carried out by only four gene products. Viral entry and membrane fusion are mediated by the envelope glycoprotein (GP), which allows the release of the viral genome into the cytoplasm, where it is transcribed in an ambisense fashion and replicated by the RNA-dependent RNA-polymerase L, in conjunction with the nucleoprotein (NP) [5]. The newly replicated small (S) and large (L) viral gene segments form ribonucleoprotein (RNP) complexes with NP and L. The viral matrix protein (Z) is composed primarily of a really interesting new gene (RING) domain and associates with both the RNPs and the glycoprotein, facilitating the formation of new virus particles [6-9]. Like many other enveloped viruses, the arenavirus matrix protein is multi-functional and provides the driving force for virus budding, as it has been shown to be both necessary and sufficient to drive the release of virus-like particles (VLPs) [10-12]. Z also mediates the recruitment of cellular machinery that carries out membrane scission, the endosomal sorting complex required for transport (ESCRT), through its late-domain motifs. JUNV Z contains a PTAP domain near its C terminus, and we have recently demonstrated that an intact ESCRT pathway is required for efficient release of infectious virus [13]. In contrast, LCMV Z contains a C-terminally located PPPY domain that, along with an intact ESCRT pathway, is dispensable for the formation of infectious virus but required to produce defective interfering particles [14]. While recent work has elucidated some of the molecular details [15], little is known about the intracellular localization of arenavirus Z during the course of infection. In particular, the cellular compartment(s) utilized or co-opted by the matrix protein to drive efficient viral assembly are unknown.

Herein, to aid in our investigations of the multifunctional role of the arenavirus matrix protein, we developed tools for the field in the form of recombinant LCMV strain Armstrong 53b or JUNV strain Candid #1 viruses that encode an HA-tagged matrix protein. In particular, we developed these viruses to address the current paucity of high-quality antibodies needed to purify or visualize Z in the setting of live virus

Received 3 November 2017; Accepted 22 December 2017

Author affiliations: [1]Department of Medicine, Division of Immunobiology, University of Vermont, Burlington, VT 05405, USA; [2]Cellular, Molecular, and Biomedical Sciences Graduate Program, University of Vermont, Burlington, VT 05405, USA; [3]Department of Microbiology and Molecular Genetics, University of Vermont, Burlington, VT 05405, USA.

***Correspondence:** Jason W. Botten, jbotten@uvm.edu

Keywords: arenavirus; lymphocytic choriomeningitis (LCMV); Junín (JUNV); Matrix protein (Z); HA epitope tag; Rab5c.

Abbreviations: ANOVA, analysis of variance; ESCRT, endosomal sorting complex required for transport; GP, glycoprotein; HA, haemagglutinin; p.i., post-infection; IP, immunoprecipitated; JUNV, Junín virus; L, RNA-dependent RNA polymerase; LASV, Lassa virus; LCMV, lymphocytic choriomeningitis virus; MOI, multiplicity of infection; NP, nucleoprotein; RING, really interesting new gene; RNP, ribonucleoprotein; TCRV, Tacaribe virus; VLP, virus-like particle; Z, matrix protein.

†These authors contributed equally to this work.

infection. The HA epitope tag was fused directly to the C terminus of LCMV (nearly adjacent to the PPPY late domain, which is located two amino acids before the end of the wild-type protein) (Fig. 1a). For JUNV, we added a spacer sequence of two alanine residues in-between the Z protein and the HA tag to avoid artificially introducing a PPPY late-domain motif, as JUNV Z terminates in a PPP sequence and the HA tag begins with a tyrosine (Fig. 1a). Pol-I vRNA expression plasmids for the small (S) segment and the large (L) segment that introduced a C-terminal HA epitope tag on Z were transiently transfected into cells, along with protein expression constructs driving the expression of the NP and L proteins; infectious virus was rescued as described in [14, 16, 17] (Fig. 1a). Viruses derived from this reverse-genetics method were rescued in parallel to wild-type Z constructs. In both cases, Z-HA tagged viruses were readily recovered; adding a tag to Z did not ablate the ability of either virus to plaque. The plaques formed by rLCMV Z-HA were smaller than wild-type (WT) LCMV (rLCMV WT) (Fig. 1b), while the plaques formed by rJUNV Z-HA were slightly larger than WT JUNV (rJUNV WT) (Fig. 1c). We examined the fitness of the tagged viruses in a multicycle growth assay. Both viruses were capable of sustained growth over multiple rounds of infection in A549 cells, with the levels being equivalent to those seen in the respective wild-type viruses at each time point. The similarity in tagged versus wild-type virus growth for both rLCMV and rJUNV strongly suggests that there is no major defect in Z's ability to carry out its normal role during the course of infection for either rLCMV Z-HA (Fig. 1d) or rJUNV Z-HA (Fig. 1e).

Having confirmed that the addition of an epitope tag did not impede viral growth, we next wanted to verify that the tag would permit robust affinity purification of Z from infected cells and/or virus particles. Accordingly, Vero E6 and A549 cells were infected with rLCMV Z-HA (Fig. 2a) or rJUNV Z-HA (Fig. 2b) at an m.o.i. of 0.01. Infected or uninfected (mock) cells and virus-containing supernatant were collected at 72 h p.i. Protein bands corresponding to both LCMV and JUNV Z-HA could be detected by an HA antibody in Vero E6 and A549 cells, but polyclonal antibodies against the respective matrix proteins were only able to detect Z in Vero E6 cells by Western blot (Fig. 1a, b), likely due to greater protein production in Vero cells and increased sensitivity of the HA antibody over the Z polyclonals. Accordingly, cell lysates and virus-containing supernatants from Vero E6 cells were incubated with a monoclonal antibody recognizing the HA epitope tag for 5 h. HA complexes were captured on protein G-coated magnetic beads by overnight incubation, extensively washed, and probed via dual-colour Western blot with antibodies against the HA epitope tag, the LCMV Z protein or the JUNV Z protein. A single protein band of the expected molecular weight was detected by both the HA- and LCMV Z-specific antibodies in cellular lysates and affinity-purified cell lysates. A band of the expected size was detected with the HA antibody in affinity-purified supernatants from infected but not mock-infected cells (Fig. 2a). While again we did not detect this protein species with the LCMV Z-specific antibody, we predict that this was due to the greater sensitivity of the HA antibody, as we have previously only been able to detect LCMV Z in virions after both concentration and immunoprecipitation [14, 18]. We observed similar results with the JUNV Z-HA protein, with a band of the predicted molecular weight being detected in both infected cells and affinity purified lysates. In the case of affinity-purified JUNV-containing supernatants, we were able to faintly detect the matrix protein with an antibody against JUNV Z, although this band was more robustly detected with an antibody against the HA tag (Fig. 2b).

Next, we investigated whether the presence of an HA tag would permit the visualization of the LCMV and JUNV matrix proteins by immunofluorescent microscopy. While previous studies have looked at the intracellular localization of LCMV and JUNV Z, the dearth of commercially available antibodies to Z and the lack of replication-competent tagged viruses have restricted research in this area. We used the tagged viruses generated in this study to infect A549 cells at an m.o.i. of 0.01 for 48 h, before fixing cells and co-staining for NP and HA as previously described [19]. As expected, signal was detected with both the anti-NP and anti-HA monoclonal antibodies in cells infected with LCMV (Fig. 2c) or JUNV (Fig. 2d). The specificity of the Z-HA staining for both viruses was confirmed by the absence of signal in identically treated and imaged uninfected (mock) cells. We observed a range of localization patterns for both NP and Z in LCMV-infected cells, likely due to the asynchronous infection necessitated by a low multiplicity of infection (Fig. 2c). LCMV in particular produces a high level of defective interfering particles, which prevents a high-multiplicity synchronous infection [20, 21]. Due to the phenotypic heterogeneity of the resulting asynchronous infections, further studies will be required to follow the localization of Z through the complete viral life cycle, as it is highly likely that Z's distribution is dynamic over the course of any given cell's infection. During the snapshot observed for this study, however, both NP and Z appeared to be primarily located in the cytoplasm, with localization patterns ranging from diffuse to punctate, with accumulations at a perinuclear location as well as in cytoplasmic puncta. We observed a limited amount of Z localized to the plasma membrane, although this enrichment was not observed for NP. While we noted the colocalization of NP and Z in what have previously been termed 'cytoplasmic inclusion bodies' [22] (see inset), these structures did not occur in every cell. In addition to cells containing such structures, we also observed populations of cells that displayed diffuse localization patterns of NP and/or Z, as well as those with distinct perinuclear or cytoplasmic puncta of either NP or Z protein that did not colocalize with each other. This compartment may be a conserved feature of Old World arenavirus assembly, as other studies have confirmed colocalization between NP and Z in specific cytoplasmic compartments in cells transiently expressing Lassa (LASV) or Mopeia virus proteins [22, 23]. Furthermore, the myristoylation at the G2 residue in Z generally required for virus-like particle release is also required for the localization of the LASV matrix protein

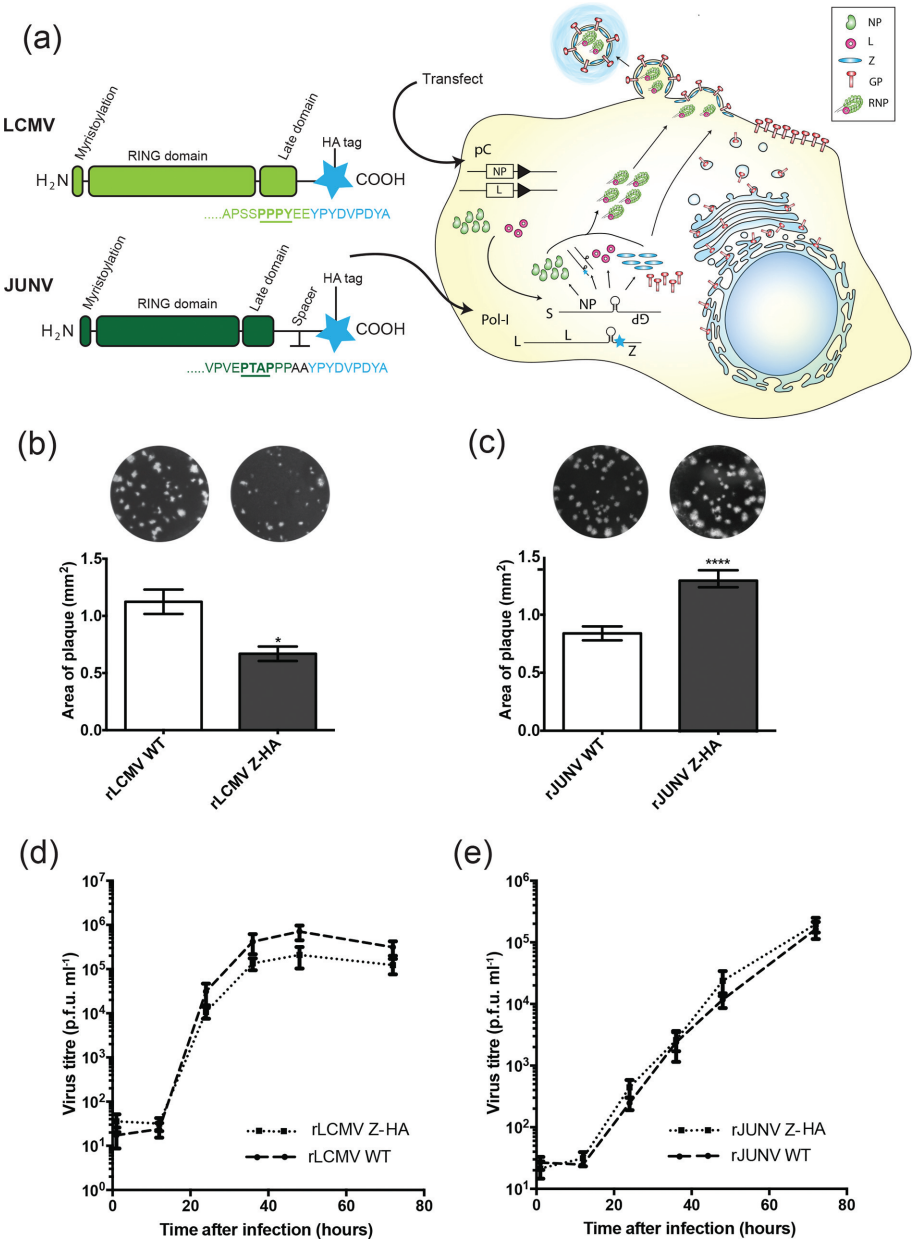

Fig. 1. Generation and characterization of arenaviruses containing HA-tagged Z protein. (a) Schematic depicting the introduction of the HA tag and the location of other important motifs in the LCMV (light green) and JUNV (dark green) matrix protein and the generation of tagged viruses by reverse genetics. Recombinant viruses were recovered following the transfection of BHK-21 cells with Pol-I vRNA expression plasmids encoding the small (S) and large (L) gene segments containing the indicated tag (blue star), along with pC protein expression plasmids for NP and L (note that while plasmid transcription occurs in the nucleus, this step is omitted from the schematic for simplicity). (b, c) The plaque size of viruses encoding HA-tagged Z proteins was determined by measuring the area of plaques formed in a standard plaque assay by rLCMV Z-HA (b) or rJUNV Z-HA (c) compared to their WT parent viruses using ImageJ. The graphs represent the mean±SEM of seven (b) or nine (c) wells from each virus, while representative images of each virus are shown. The mean values were compared using the Mann–Whitney non-parametric test. (d, e) A549 cells infected at a multiplicity of infection (m.o.i.) of 0.01 were used to assess the kinetics of virus propagation via growth curve analysis. The data represent the mean ±SEM of three independent experiments and statistical analyses were performed using a two-way ANOVA with Holm–Sidak's test for multiple comparisons on log-transformed data. *P<0.05, ****P<0.0001 for the indicated statistical tests. In the absence of indicated asterisks, no significant difference was detected.

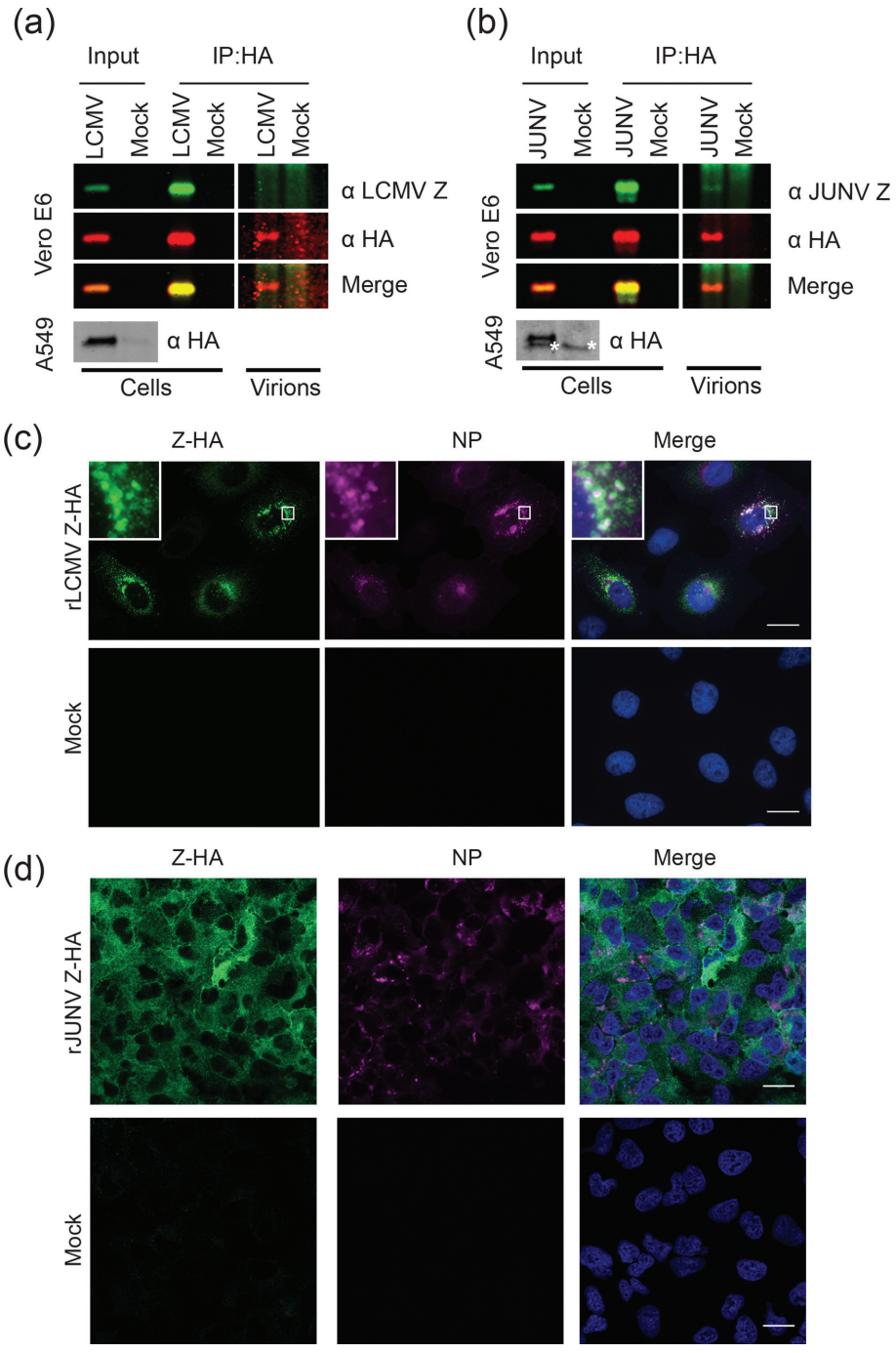

Fig. 2. Biochemical validation and visualization of arenaviruses encoding an epitope-tagged Z protein. (a, b) Vero E6 or A549 cells were infected with rLCMV Z-HA (a) or rJUNV Z-HA (b) at an m.o.i. of 0.01. Three days later the cells (Vero E6 and A549s) and virus-containing media (Vero E6) were collected and lysed in Triton lysis buffer (Input). HA-tagged Z protein from Vero E6 cells was immunoprecipitated (IP) from cells and virus-containing supernatants using a mouse anti-HA antibody (Covance, MMS-101P) and protein G-coated magnetic beads. Z was detected by Licor two-colour fluorescent Western blotting using antibodies to HA and rabbit immunosera to either LCMV Z (a) [antibody (880), generously provided by M.J. Buchmeier] or JUNV Z (b) (generously provided by Dr Sandra Goñi [46]). A background band detected in A549 cells by the HA antibody is identified by an asterisk. (c, d) Single slices of either mock- or rLCMV Z-HA-infected (c) or rJUNV Z-HA-infected (d) A549 cells at 48 h p.i. that were stained for viral nucleoprotein (NP) (mouse anti-LCMV NP 1–1.3; BEI Resources, mouse anti-JUNV NP NA05-AG12) and HA (Abcam, ab9110) are shown. The perinuclear region of interest in rLCMV Z-HA-infected cells (white box) is enlarged (inset). Scale bars, 20 µm.

at cytoplasmic aggregate structures, as well as the plasma membrane [24, 25]. While we did not observe colocalization of NP and Z in this compartment in every cell, it is possible that this structure is formed transiently during a particular step of the life cycle (especially as the necessity of a multicycle, low m.o.i. infection results in an asynchronous population of infected cells). Alternatively, it is possible that the presence of cells in which NP and Z do not appear to colocalize is an LCMV-specific feature that distinguishes it from LASV and Mopeia.

Cells infected with rJUNV Z-HA displayed a more uniform distribution of both NP and Z-HA (Fig. 2d). At 48 h p.i. JUNV Z-HA was observed primarily in a diffuse cytoplasmic localization pattern, with some plasma membrane staining and a perinuclear accumulation seen in a minority of cells. The localization of JUNV Z described above is also in accordance with previous reports that examined the localization of JUNV Z expressed from plasmid [26-28]. JUNV NP appeared to be concentrated primarily in distinct cytoplasmic structures, as expected from previous studies

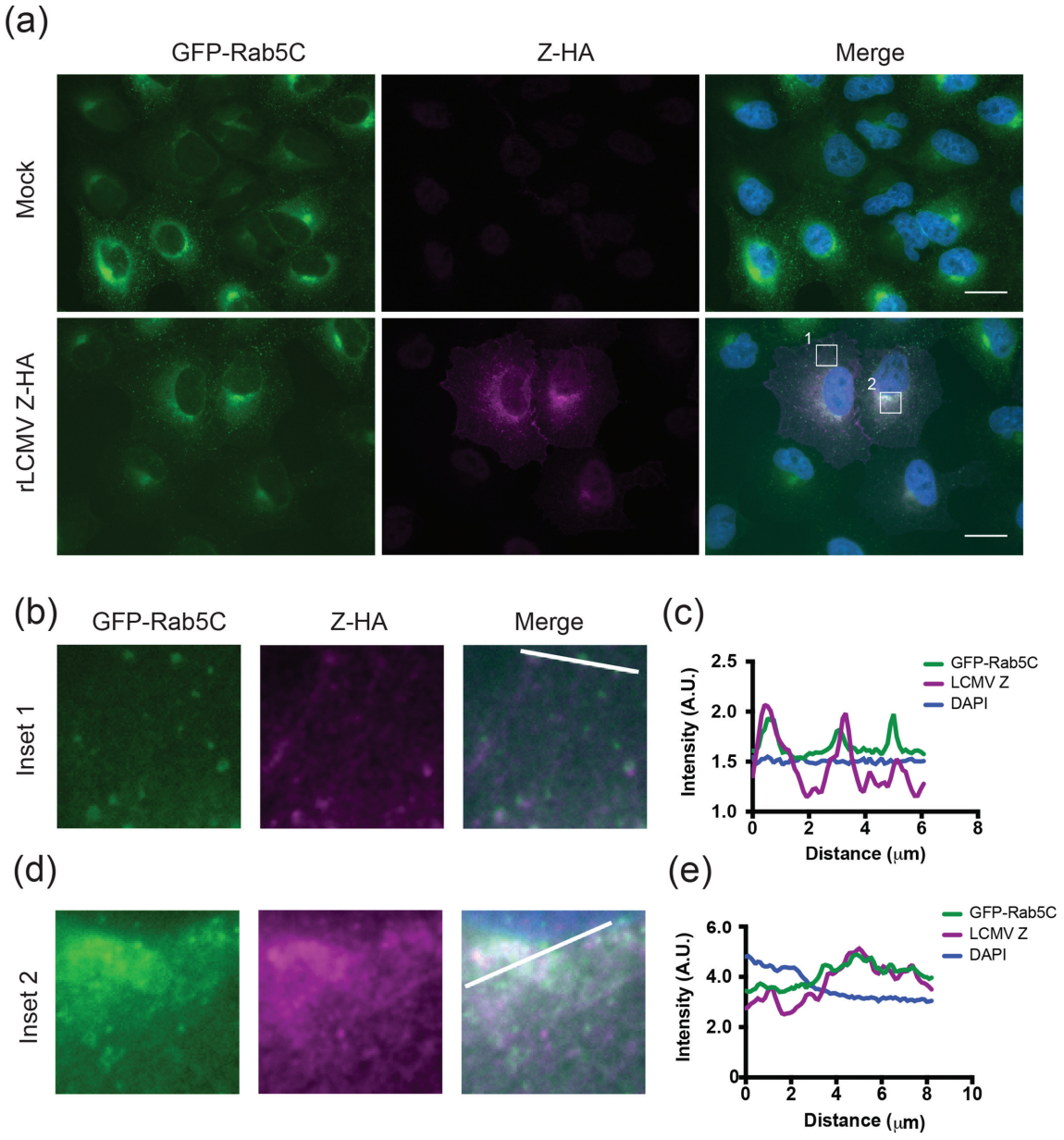

Fig. 3. LCMV Z and Rab5c colocalize in a perinuclear location and cytoplasmic vesicles. (a) Single slices of either mock- or rLCMV Z-HA-infected A549 cells stably expressing GFP-Rab5c (48 h p.i.) stained with HA antibody (Abcam, ab9110) are shown. (b, d) Cytoplasmic (inset 1, b) and perinuclear (inset 2, d) regions of interest are enlarged. (c, e). Fluorescence line scan of GFP-Rab5c, Z-HA and DAPI signals along the line indicated in the insets in (b, d). Scale bars, 20 μm.

[19, 29]. Studies with another New World virus, Tacaribe (TCRV), showed a similar localization pattern for plasmid-expressed Z [28, 30], although the assembly and budding processes of TCRV may not be generalizable to other New World arenaviruses, as TCRV Z lacks a canonical PT/SAP late-domain and NP significantly enhances the budding activity of TCRV Z in VLP assays [31]. The lack of overt colocalization between JUNV Z and NP may reflect a difference in viral assembly between New and Old World arenaviruses, although to our knowledge this is the first report of Z's distribution in JUNV-infected cells. The exact vesicular and motor proteins required to traffic viral components to the site(s) of assembly and budding are still being elucidated, although recent work has shown that the microtubule motor protein Kif13A colocalizes with both LASV and JUNV Z [15]. The ability to image Old and New World arenavirus matrix proteins in tandem with detection of the genome [32] and nucleoprotein should greatly aid this effort.

After validating our ability to image the matrix protein in both tagged viruses, we used the rLCMV Z-HA virus to infect A549 cells that we transduced to stably express low levels of GFP-Rab5c (as described in [33]). Previous work by our group and others has shown that Rab5c plays an important role in LCMV propagation, although it appears to be dispensable for JUNV replication [13, 32, 34]. It is likely that Rab5c is involved in a late step in the viral life cycle, as LCMV genomic RNA closely colocalizes with Rab5c at 48 but not 24 h p.i. [32]. Furthermore, Old World arenaviruses are thought to enter cells primarily via a Rab5-independent mechanism, although the studies showing this generally examined the role of the closely related Rab5a isoform [35-37]. As expected, we observed that GFP-Rab5c was localized in vesicular structures throughout the cytoplasm, with a concentration of protein being seen at a perinuclear location in the majority of both infected and uninfected cells (Fig. 3a). Strikingly, we noted pronounced colocalization between GFP-Rab5c and LCMV Z in both a subset of cytoplasmic vesicles (Fig. 3b, c) and a perinuclear compartment (Fig. 3d, e). Given that we have previously observed colocalization between both LCMV genomic RNA and the glycoprotein, as well as genomic RNA and Rab5c at a similar compartment during late steps of the viral life cycle [32], it appears that the assembly of at least a subset of virion components may be coordinated at a cytoplasmic location prior to budding at the plasma membrane. While further work is needed to fully elucidate the trafficking steps involved in arenavirus assembly prior to budding, there is a precedent for other negative-strand viruses co-opting cellular membrane compartments to ensure efficient trafficking of viral components, as well as coordinating their packaging into mature virions. Influenza A virus, for example, hijacks the cellular Rab11 machinery to transport its vRNPs from the nucleus to the plasma membrane [38-40]. This pathway is used not only for trafficking, but also to mediate the packaging of individual genome segments, steps which are required for the final budding step of virus particles [41-43]. Hepatitis virus also utilizes a Rab GTPase during viral assembly, as Rab18 is required to traffic the viral core protein to lipid droplets [44, 45].

In summary, we have generated novel recombinant Old and New World arenaviruses with tagged matrix proteins that are easily recoverable and grow to wild-type levels. These viruses facilitate robust affinity purification of matrix protein from cells and virus particles as well as straightforward detection by immunofluorescent microscopy. The rJUNV Z-HA virus generated in this study revealed the localization of Z in infected cells, and this is the first such report to our knowledge. We also confirmed the colocalization of LCMV Z and NP in cytoplasmic structures in a subset of infected cells. Finally, we presented one of the first descriptions of colocalization between an arenavirus matrix protein and a cellular protein (Rab5c) in infected cells. These viruses will be useful and versatile tools for the field in elucidating the precise roles that Z plays in the arenavirus life cycle.

Funding information
This publication was made possible by support from NIH grants T32 HL076122 (B. R. K. and C. M. Z.), T32 AI055402 (C. M. Z.), R21 AI088059 (J. B.), and P20RR021905 and P30GM118228 (Immunobiology and Infectious Disease COBRE awards) (J. B.).

Acknowledgements
For providing key reagents and support we gratefully acknowledge Dr Michael Buchmeier (LCMV NP antibody 1–1.3, LCMV Z antibody 880 and JUNV strain Candid #1), Dr J. Lindsay Whitton (LCMV strain Armstrong 53b and Vero E6 cells), Dr Sandra Goñi (JUNV Z antibody), Dr Felix Randow (retroviral transduction system) and Dr Ágnes Föglein (technical assistance). Wide-field fluorescent microscopy (LCMV) was carried out on a Nikon Ti-E microscopy (courtesy of Dr Jason Stumpff). Confocal microscopy (JUNV) was performed at the Microscopy Imaging Center at the University of Vermont on a Zeiss 510 META laser scanning confocal microscope supported by NIH award number 1S10RR019246 from the National Center for Research Resources.

Conflicts of interest
The authors declare that there are no conflicts of interest.

References

1. **Maiztegui JI.** Clinical and epidemiological patterns of Argentine haemorrhagic fever. *Bull World Health Organ* 1975;52:567–575.
2. **Salazar-Bravo J, Ruedas LA, Yates TL.** Mammalian reservoirs of arenaviruses. In: Oldstone MA (editor). *Arenaviruses I (Current Topics in Microbiology and Immunology*. Berlin Heidelberg: Springer; 2002. pp. 25–63.
3. **Childs JE, Glass GE, Korch GW, Ksiazek TG, Leduc JW.** Lymphocytic choriomeningitis virus infection and house mouse (*Mus musculus*) distribution in urban Baltimore. *Am J Trop Med Hyg* 1992; 47:27–34.
4. **Keenlyside RA, McCormick JB, Webb PA, Smith E, Elliott L *et al.*** Case-control study of Mastomys natalensis and humans in Lassa virus-infected households in Sierra Leone. *Am J Trop Med Hyg* 1983;32:829–837.
5. **Meyer BJ, de La Torre JC, Southern PJ.** Arenaviruses: genomic RNAs, transcription, and replication. In: Oldstone MA (editor). *Arenaviruses I (Current Topics in Microbiology and Immunology)*. Berlin Heidelberg: Springer; 2002. pp. 139–157.
6. **Fehling SK, Lennartz F, Strecker T.** Multifunctional nature of the arenavirus RING finger protein Z. *Viruses* 2012;4:2973–3011.
7. **Djavani M, Lukashevich IS, Sanchez A, Nichol ST, Salvato MS.** Completion of the Lassa fever virus sequence and identification of a RING finger open reading frame at the L RNA 5' End. *Virology* 1997;235:414–418.

8. Schlie K, Maisa A, Freiberg F, Groseth A, Strecker T *et al.* Viral protein determinants of Lassa virus entry and release from polarized epithelial cells. *J Virol* 2010;84:3178–3188.
9. Capul AA, Perez M, Burke E, Kunz S, Buchmeier MJ *et al.* Arenavirus Z-glycoprotein association requires Z myristoylation but not functional RING or late domains. *J Virol* 2007;81:9451–9460.
10. Strecker T, Eichler R, Meulen J, Weissenhorn W, Dieter Klenk H *et al.* Lassa virus Z protein is a matrix protein and sufficient for the release of virus-like particles [corrected]. *J Virol* 2003;77: 10700–10705.
11. Perez M, Craven RC, de La Torre JC. The small RING finger protein Z drives arenavirus budding: implications for antiviral strategies. *Proc Natl Acad Sci USA* 2003;100:12978–12983.
12. Eichler R, Strecker T, Kolesnikova L, ter Meulen J, Weissenhorn W *et al.* Characterization of the Lassa virus matrix protein Z: electron microscopic study of virus-like particles and interaction with the nucleoprotein (NP). *Virus Res* 2004;100:249–255.
13. Ziegler CM, Eisenhauer P, Kelly JA, Dang LN, Beganovic V *et al.* A proteomic survey of Junín virus interactions with human proteins reveals host factors required for arenavirus replication. *J Virol* 2017:JVI.01565-17.
14. Ziegler CM, Eisenhauer P, Bruce EA, Weir ME, King BR *et al.* The lymphocytic choriomeningitis virus matrix protein PPXY late domain drives the production of defective interfering particles. *PLoS Pathog* 2016;12:e1005501.
15. Fehling SK, Noda T, Maisner A, Lamp B, Conzelmann KK *et al.* The microtubule motor protein KIF13A is involved in intracellular trafficking of the Lassa virus matrix protein Z. *Cell Microbiol* 2013; 15:315–334.
16. Flatz L, Bergthaler A, de La Torre JC, Pinschewer DD. Recovery of an arenavirus entirely from RNA polymerase I/II-driven cDNA. *Proc Natl Acad Sci USA* 2006;103:4663–4668.
17. Emonet SF, Seregin AV, Yun NE, Poussard AL, Walker AG *et al.* Rescue from cloned cDNAs and *in vivo* characterization of recombinant pathogenic Romero and live-attenuated Candid #1 strains of Junin virus, the causative agent of Argentine hemorrhagic fever disease. *J Virol* 2011;85:1473–1483.
18. Ziegler CM, Eisenhauer P, Bruce EA, Beganovic V, King BR *et al.* A novel phosphoserine motif in the LCMV matrix protein Z regulates the release of infectious virus and defective interfering particles. *J Gen Virol* 2016;97:2084–2089.
19. King BR, Hershkowitz D, Eisenhauer PL, Weir ME, Ziegler CM *et al.* A map of the arenavirus nucleoprotein-host protein interactome reveals that Junín virus selectively impairs the antiviral activity of double-stranded RNA-activated protein kinase (PKR). *J Virol* 2017;91: e00763-17.
20. Welsh RM, Pfau CJ. Determinants of lymphocytic choriomeningitis interference. *J Gen Virol* 1972;14:177–187.
21. Huang AS, Baltimore D. Defective viral particles and viral disease processes. *Nature* 1970;226:325–327.
22. Ortiz-Riaño E, Cheng BY, de La Torre JC, Martínez-Sobrido L. The C-terminal region of lymphocytic choriomeningitis virus nucleoprotein contains distinct and segregable functional domains involved in NP-Z interaction and counteraction of the type I interferon response. *J Virol* 2011;85:13038–13048.
23. Shtanko O, Imai M, Goto H, Lukashevich IS, Neumann G *et al.* A role for the C terminus of Mopeia virus nucleoprotein in its incorporation into Z protein-induced virus-like particles. *J Virol* 2010; 84:5415–5422.
24. Perez M, Greenwald DL, de La Torre JC. Myristoylation of the RING finger Z protein is essential for arenavirus budding. *J Virol* 2004;78:11443–11448.
25. Strecker T, Maisa A, Daffis S, Eichler R, Lenz O *et al.* The role of myristoylation in the membrane association of the Lassa virus matrix protein Z. *Virol J* 2006;3:93.
26. García CC, Ellenberg PC, Artuso MC, Scolaro LA, Damonte EB. Characterization of Junín virus particles inactivated by a zinc finger-reactive compound. *Virus Res* 2009;143:106–113.
27. Fan L, Briese T, Lipkin WI. Z proteins of New World arenaviruses bind RIG-I and interfere with type I interferon induction. *J Virol* 2010;84:1785–1791.
28. Loureiro ME, Wilda M, Levingston Macleod JM, D'Antuono A, Foscaldi S *et al.* Molecular determinants of Arenavirus Z protein homo-oligomerization and L polymerase binding. *J Virol* 2011: JVI.05691-05611.
29. Baird NL, York J, Nunberg JH. Arenavirus infection induces discrete cytosolic structures for RNA replication. *J Virol* 2012;86: 11301–11310.
30. Levingston Macleod JM, D'Antuono A, Loureiro ME, Casabona JC, Gomez GA *et al.* Identification of two functional domains within the arenavirus nucleoprotein. *J Virol* 2011;85:2012–2023.
31. Groseth A, Wolff S, Strecker T, Hoenen T, Becker S. Efficient budding of the tacaribe virus matrix protein z requires the nucleoprotein. *J Virol* 2010;84:3603–3611.
32. King BR, Kellner S, Eisenhauer PL, Bruce EA, Ziegler CM *et al.* Visualization of the lymphocytic choriomeningitis mammarenavirus (LCMV) genome reveals the early endosome as a possible site for genome replication and viral particle pre-assembly. *J Gen Virol* 2017;98:2454–2460.
33. Randow F, Sale JE. Retroviral transduction of DT40. *Subcell Biochem* 2006;40:383–386.
34. Panda D, Das A, Dinh PX, Subramaniam S, Nayak D *et al.* RNAi screening reveals requirement for host cell secretory pathway in infection by diverse families of negative-strand RNA viruses. *Proc Natl Acad Sci USA* 2011;108:19036–19041.
35. Rojek JM, Kunz S. Cell entry by human pathogenic arenaviruses. *Cell Microbiol* 2008;10:828–835.
36. Pasqual G, Rojek JM, Masin M, Chatton JY, Kunz S. Old world arenaviruses enter the host cell via the multivesicular body and depend on the endosomal sorting complex required for transport. *PLoS Pathog* 2011;7:e1002232.
37. Quirin K, Eschli B, Scheu I, Poort L, Kartenbeck J *et al.* Lymphocytic choriomeningitis virus uses a novel endocytic pathway for infectious entry via late endosomes. *Virology* 2008;378:21–33.
38. Amorim MJ, Bruce EA, Read EK, Foeglein A, Mahen R *et al.* A Rab11- and microtubule-dependent mechanism for cytoplasmic transport of influenza A virus viral RNA. *J Virol* 2011;85:4143–4156.
39. Momose F, Sekimoto T, Ohkura T, Jo S, Kawaguchi A *et al.* Apical transport of influenza A virus ribonucleoprotein requires Rab11-positive recycling endosome. *PLoS One* 2011;6:e21123.
40. Eisfeld AJ, Kawakami E, Watanabe T, Neumann G, Kawaoka Y. RAB11A is essential for transport of the influenza virus genome to the plasma membrane. *J Virol* 2011;85:6117–6126.
41. Chou YY, Heaton NS, Gao Q, Palese P, Singer RH *et al.* Colocalization of different influenza viral RNA segments in the cytoplasm before viral budding as shown by single-molecule sensitivity FISH analysis. *PLoS Pathog* 2013;9:e1003358.
42. Lakdawala SS, Wu Y, Wawrzusin P, Kabat J, Broadbent AJ *et al.* Influenza a virus assembly intermediates fuse in the cytoplasm. *PLoS Pathog* 2014;10:e1003971.
43. Bruce EA, Digard P, Stuart AD. The Rab11 pathway is required for influenza A virus budding and filament formation. *J Virol* 2010;84: 5848–5859.
44. Dansako H, Hiramoto H, Ikeda M, Wakita T, Kato N. Rab18 is required for viral assembly of hepatitis C virus through trafficking of the core protein to lipid droplets. *Virology* 2014;462-463:166–174.
45. Salloum S, Wang H, Ferguson C, Parton RG, Tai AW. Rab18 binds to hepatitis C virus NS5A and promotes interaction between sites of viral replication and lipid droplets. *PLoS Pathog* 2013;9: e1003513.
46. Goñi SE, Borio CS, Romano FB, Rota RP, Pilloff MG *et al.* Expression and purification of Z protein from Junín virus. *J Biomed Biotechnol* 2010;2010:1–14.